Atmospheric
Chemistry
and Physics

Measurements of total hydroxyl radical reactivity during CABINEX 2009 – Part 1: field measurements

R. F. Hansen[1,2,*], **S. M. Griffith**[2,3], **S. Dusanter**[3,4,5], **P. S. Rickly**[2,3], **P. S. Stevens**[1,2,3], **S. B. Bertman**[6], **M. A. Carroll**[7,8], **M. H. Erickson**[9], **J. H. Flynn**[10], **N. Grossberg**[10], **B. T. Jobson**[9], **B. L. Lefer**[10], and **H. W. Wallace**[9]

[1]Department of Chemistry, Indiana University, Bloomington, IN, USA
[2]Center for Research in Environmental Science, Indiana University, Bloomington, IN, USA
[3]School of Public and Environmental Affairs, Indiana University, Bloomington, IN, USA
[4]Mines Douai, CE, F59508, Douai, France
[5]Université Lille Nord de France, 59000, Lille, France
[6]Department of Chemistry, Western Michigan University, Kalamazoo, MI, USA
[7]Department of Chemistry, University of Michigan, Ann Arbor, MI, USA
[8]Department of Atmospheric, Oceanic, and Space Sciences, University of Michigan, Ann Arbor, MI, USA
[9]Department of Civil and Environmental Engineering, Washington State University, Pullman, WA, USA
[10]Department of Earth and Atmospheric Sciences, University of Houston, Houston, TX, USA
[*]now at: School of Chemistry, University of Leeds, Woodhouse Lane, Leeds, LS2 9JT, UK

Correspondence to: R. F. Hansen (rfhansen@indiana.edu)

Abstract. Total hydroxyl radical (OH) reactivity was measured at the PROPHET (Program for Research on Oxidants: PHotochemistry, Emissions, and Transport) forested field site in northern Michigan during the 2009 Community Atmosphere–Biosphere INteraction EXperiment (CABINEX). OH reactivity measurements were made with a turbulent-flow reactor instrument at three heights from the forest floor above (21 and 31 m) and below (6 m) the canopy at three different time periods during the CABINEX campaign. In addition to total OH reactivity measurements, collocated measurements of volatile organic compounds (VOCs), inorganic species, and ambient temperature were made at the different heights. These ancillary measurements were used to calculate the total OH reactivity, which was then compared to the measured values. Discrepancies between the measured and calculated OH reactivity, on the order of $1–24\,s^{-1}$, were observed during the daytime above the canopy at the 21 and 31 m heights, as previously reported for this site. The measured OH reactivity below the canopy during the daytime was generally lower than that observed above the canopy. Closer analysis of the measurements of OH reactivity and trace gases suggests that the missing OH reactivity could

come from oxidation products of VOCs. These results suggest that additional unmeasured trace gases, likely oxidation products, are needed to fully account for the OH reactivity measured during CABINEX.

1 Introduction

The hydroxyl radical (OH) is an important oxidant in the troposphere. OH controls the chemical lifetimes of many important atmospheric trace gases (Ehhalt, 1998) and is also involved in the formation of tropospheric ozone and secondary organic aerosols. Because of the key role that OH plays in tropospheric chemistry, an accurate understanding of OH sources and sinks is important. Due to its high reactivity, there are numerous sinks of OH in the atmosphere. Among the most important are nitrogen oxides and volatile organic compounds (VOCs). However, of the hundreds of possible VOCs within the atmosphere, many still elude detection by traditional VOC measurement techniques (Goldstein and Galbally, 2007). Thus, a complete characterization of all the individual OH sinks is a daunting task. One way to

characterize OH sinks without the need for measurements of their concentrations is to directly measure the total OH loss rate due to chemical reactions through measurements of the total OH reactivity.

The OH reactivity (k_X) is defined for a chemical species X as the product of the second-order rate constant (or, for termolecular reactions, the bimolecular rate constant calculated at the working pressure) for the reaction of X with OH ($k_{X,OH}$) and the concentration of X:

$$k_X = k_{X,OH}[X]. \tag{1}$$

The total OH reactivity k_{OH}, which is the inverse of the OH lifetime, can be derived by summing the OH reactivity for each chemical species X_i:

$$k_{OH} = \sum_i k_{X_i,OH}[X_i]. \tag{2}$$

Instruments to measure ambient total OH reactivity have been recently developed and deployed in several field campaigns (Lou et al., 2010; Dolgorouky et al., 2012; Nölscher et al., 2012; Sinha et al., 2012). These instruments employ one of three methods, all of which measure the OH reactivity by mixing ambient air with a large amount of OH in a sampling reactor and monitoring the change in the concentration of OH or a tracer molecule. The first method, known as the total OH loss rate method (TOHLM) (Kovacs and Brune, 2001; Ingham et al., 2009), uses a flow tube reactor with a movable OH injector coupled to a laser-induced fluorescence detection cell (fluorescence assay with gas expansion, FAGE). A second method, the dual-laser pump-probe method (Sadanaga et al., 2004b), employs one laser for OH generation at 266 nm from the photolysis of ambient O_3 in the sampling reactor and a laser-induced fluorescence detection cell (FAGE) to probe OH. Both methods rely on the direct detection of OH to measure the first-order OH loss rate. The third method, known as the comparative reactivity method (CRM) (Sinha et al., 2008), is an indirect method in which a tracer molecule is detected instead of OH to determine the ambient OH loss rate.

Direct measurements of total OH reactivity from any one of these techniques can be compared to values calculated via Eq. (2) from measured concentrations of known OH sinks to assess whether unmeasured trace gases are important unaccounted OH sinks. The difference between the measured and calculated total OH reactivity is referred to as the "missing" OH reactivity and represents the loss of OH from unmeasured sinks.

Missing OH reactivity analyses have been conducted for several urban and forested areas. The agreement between measured and calculated total OH reactivity in urban areas has generally been good, with missing OH reactivity of less than $3\,s^{-1}$ (5–10 % of the measured total OH reactivity), well within the combined uncertainties of the OH reactivity measurements and the OH reactivity calculations (Ren et

al., 2003a; Di Carlo et al., 2004; Mao et al., 2010). However, some missing OH reactivity on the order of 5–$30\,s^{-1}$ (10–50 % of the total) has been seen sometimes in Nashville (Kovacs et al., 2003), New York City (Ren et al., 2006a), and Tokyo (Chatani et al., 2009; Sadanaga et al., 2004a; Yoshino et al., 2006).

In contrast, the agreement between calculated and measured total OH reactivity has been poorer in forested environments (Table 1). Previous measurements of OH reactivity made at the PROPHET (Program for Research on Oxidants: PHotochemistry, Emissions, and Transport) site in northern Michigan found missing OH reactivity values between 1 and $4\,s^{-1}$ (33–50 % of the total) that exhibited a clear dependence on temperature (Di Carlo et al., 2004). OH reactivity measurements in a coniferous forest in California also found significant missing OH reactivity that also displayed a temperature dependence, although the absolute values were higher (2.5–$10\,s^{-1}$, 30–40 % of the total) (Mao et al., 2012). Even higher missing OH reactivity ($36\,s^{-1}$, 68 % of the total) was measured in a rainforest in Suriname in 2005 (Sinha et al., 2008). The magnitude of missing OH reactivity from a boreal forest in Finland was less, being only $4.6\,s^{-1}$ on average, but this accounted for 50 % of the total OH reactivity in this environment (Sinha et al., 2010). Similar results were obtained at the same site in 2010, with $8.9\,s^{-1}$ of missing reactivity on average comprising 77 % of the total OH reactivity (Nölscher et al., 2012).

Of all the studies of OH reactivity conducted in forested environments (summarized in Table 1), only one study does not report significant missing OH reactivity (Ren et al., 2006b). This study was conducted in a deciduous forest in eastern New York State, which is influenced by urban air masses. It is unclear why no significant missing OH reactivity was observed at this site, although the median contribution of isoprene to OH reactivity was only 14 % (Ren et al., 2006b). In other campaigns conducted in forested areas, the measured OH reactivity has been at least 50 % higher than the OH reactivity calculated from measured trace species. This missing reactivity has been attributed to undetected emissions of highly reactive biogenic VOCs (BVOCs; Di Carlo et al., 2004; Sinha et al., 2010), unmeasured VOC oxidation products (Edwards et al., 2013; Lou et al., 2010; Mao et al., 2012), or combinations of these two (Nölscher et al., 2012).

Most of the OH reactivity measurements to date within forested environments have been made above the forest canopy (see Table 1). As locally emitted VOCs and their oxidation products, trace gases carried by transport, and solar radiation are all present above the canopy, this environment is expected to be the most chemically active within the forest. However, Holzinger et al. (2005) have observed VOC oxidation products both above and below a forest canopy, indicating that the below-canopy OH reactivity may also provide useful information to investigate potential sources of missing OH reactivity. One-dimensional modeling by Mogensen

Table 1. Summary of total OH reactivity measurements in forested environments.

Campaign	Site	Dates	Forest type	z_{meas}/z_c[a]	MR[b]	k_{OH} (s^{-1})[c]	Tech.[d]	Reference
PROPHET 2000	Michigan, USA	Jul–Aug 2000	Mixed deciduous	1.5	~ 1.5	1–12[e]	T	Di Carlo et al. (2004)
PMTACS	Whiteface Mountain, NY, USA	Jul–Aug 2002	Mixed deciduous	[f]	~ 1	3–12	T	Ren et al. (2006b)
(N/A)	Brownsberg, Suriname	Oct 2005	Rainforest	0.88	~ 3.5	30–70	C	Sinha et al. (2008)
OP-3	Borneo, Malaysia	Apr–May 2008	Rainforest	[g]	~ 3[h]	5–80	T	Edwards et al. (2013)
SMEAR/ BFORM	Hyytiälä, Finland	Aug 2008	Boreal	0.86	$\sim 3-4$[i]	3–30	C	Sinha et al. (2010)
BEARPEX 2009	California, USA	Jun–Jul 2009	Coniferous	1–1.7[j]	~ 1.5	8-25[e]	T	Mao et al. (2012)
HUMPPA-COPEC 2010	Hyytiälä, Finland	Jul–Aug 2010	Boreal	0.87[k]	[l]	3–76	C	Nölscher et al. (2012)
				1.17[k]	5.22[m]	3–60	C	
CABINEX	Michigan, USA	Jul–Aug 2009	Mixed deciduous	0.32[p]	2.26[q]	1–39	T	This work
				1.1[p]	2.07[q]	1–39	T	
				1.63[p]	2.34[q]	1–42	T	

[a] Ratio of measurement height to average canopy height. [b] Missing reactivity fraction: ratio of total measured OH reactivity to total calculated OH reactivity. [c] Range of individual OH reactivity measurements for entire campaign, unless otherwise indicated. [d] Measurement technique used: T = total OH loss rate method; C = comparative reactivity method. [e] Range of temperature-binned averages. [f] Measurements made in canopy, no measurement height given. [g] Measurement made in a forest clearing at a height of 5 m. [h] Calculated from diurnal average at ~ 15:00 LT. [i] Median value: missing reactivity fractions ranged from 1 to 12. [j] Measurements at multiple heights (9, 12 and 15 m), combined for analysis. [k] Measurements from multiple heights (18 and 24 m). [l] Calculated OH reactivity from in-canopy measurements not reported. [m] Calculated from whole-campaign average values. [p] Measurements from multiple heights (6, 21, and 31 m). [q] Median values.

et al. (2011) shows that ambient OH reactivity can vary with height in a forest environment. These observations motivate further measurements both within and below the forest canopy.

The Community Atmosphere–Biosphere INteraction EXperiment (CABINEX) campaign during the summer of 2009 provided an opportunity to measure OH reactivity at multiple heights within a forest canopy where previous measurements from this site highlighted significant missing OH reactivity above the canopy at a height of 29 m (Di Carlo et al., 2004). This paper presents measurements of total OH reactivity at three heights (6, 21, and 31 m) above the floor of a mixed deciduous forest. The measurements made below the canopy at 6 m and above the canopy at 21 and 31 m have been analyzed and compared to OH reactivity values calculated from collocated measurements of VOCs and inorganic trace species to confirm whether missing OH reactivity is observed above the canopy and to gain insights into processes that could lead to some missing OH reactivity at this site.

2 Experimental

2.1 Instrument description

The total OH reactivity instrument used for these measurements is based on the total OH loss rate method (TOHLM) (Kovacs and Brune, 2001), which itself is an adaptation of the flow-discharge technique used in kinetic studies (Seeley et al., 1993). The Indiana University instrument (IU-TOHLM) consists of three major components (Fig. 1): a movable OH radical source, a flow tube reactor, and an OH radical detection system that is connected to the flow tube reactor through an adapter block.

The flow tube reactor consists of a 5 cm-i.d. (inner diameter) glass tube that is 75 cm in length with several 1.2 cm-o.d. (outer diameter) ports (at 25 cm intervals) along the length of the tube. At the upstream end of the reactor, there are two 5 cm-o.d. intake arms perpendicular to each other. Ambient

air is introduced through the intake arm perpendicular to the main axis of the reactor. To determine the loss rate of OH due to wall reactions in the flow tube (k_b), high-purity nitrogen from a liquid nitrogen dewar (Indiana Oxygen, industrial grade for laboratory measurements; Airgas, 99.999 % purity for field measurements) is introduced through an intake arm perpendicular to the main axis of the reactor (Fig. 1). The OH radical source injector is inserted along the main axis of the reactor (Fig. 1). The gas velocity is measured near the exit of the flow tube reactor with a Pitot-static tube (Dwyer Instruments 167-6) connected to a 0–1.8 torr differential pressure gauge (Omega Instruments PX654-015DV). The end of the Pitot tube is placed within the reactor facing the opposite direction of the main flow, approximately 1 cm away from the reactor wall at a distance of 4.5 cm upstream of the OH detection system. This places the Pitot tube within the turbulent core region of the reactor. Since the OH detection axis, due to its orientation relative to the flow tube, samples preferentially from the turbulent core region, the flow velocity should be measured in this region for accurate kinetic measurements (Seeley et al., 1993). To confirm the accuracy of flow velocity measurements, the Pitot tube was collocated with a portable hot-wire anemometer (Testo v 405), and standard flows of nitrogen (40–200 L min^{-1}) were passed through the flow tube. The flow velocity measurements made using the anemometer and the Pitot tube were within 10 % of each other. To measure the temperature of the air inside the flow tube, a thermocouple was placed inside the flow tube within a port closest to the exit, approximately 12 cm from the exit of the flow tube.

The OH radical source injector consists of a mercury pen lamp (UVP Pen-Ray) housed in a 2 m-long, 1.25 cm-o.d. stainless steel tube. The top of the mercury pen lamp is positioned approximately 1 cm upstream of the exit of the injector. On the downstream end of the injector, there is an aluminum cap with small holes drilled concentrically with an approximately 60° angle of coverage to promote the mixing of OH radicals with the main flow. In addition to enhancing mixing of OH radicals within the reactor, this cap
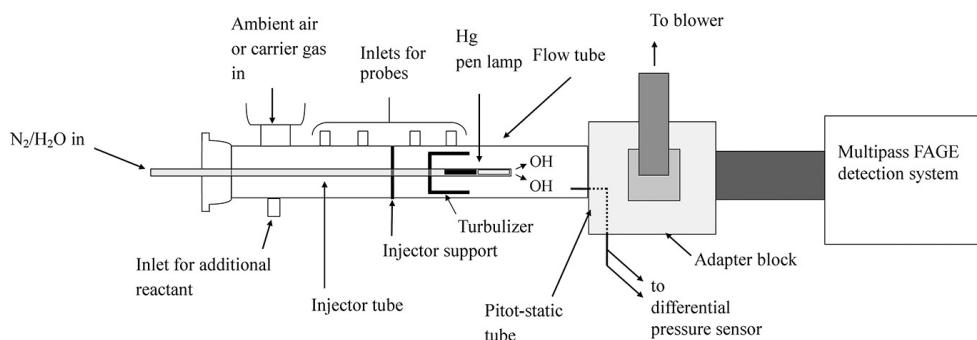
Fig. 1. Diagram of the IU-TOHLM instrument.

also minimizes the dispersion of ultraviolet radiation into the reactor, where some ambient trace species could be photolyzed. A turbulizer, made of Teflon and consisting of four 1 cm-wide fins placed at 90° angles along the circumference of the flow tube, is attached to the injector 10 cm upstream of the cap to help promote mixing and to help establish turbulent flow conditions (Seeley et al., 1993).

To generate OH radicals, a 5–$10\,L\,min^{-1}$ flow of nitrogen is bubbled through high-purity water (EMD Chemicals), producing a humid flow of carrier gas. The water vapor is then photolyzed by the 185 nm emission from the mercury lamp, producing approximately equal concentrations of OH and H atoms.

$$H_2O + h\nu(185\,nm) \longrightarrow H\cdot + OH\cdot \quad (R1)$$
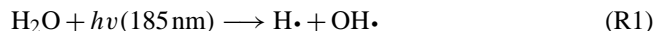
The H atoms produced from reaction R1 can then react rapidly with molecular oxygen present as an impurity in the carrier gas to produce HO_2 radicals. Any unreacted H atoms leaving the injector would react with ambient O_2 to form HO_2 radicals due to the large excess of oxygen in air compared to trace gases.

$$H\cdot + O_2 + M \longrightarrow HO_2\cdot + M \quad (R2)$$

Under field measurement conditions, it was determined through calibration of the OH detection axis (Dusanter et al., 2008) that the initial concentration of OH radicals in the reactor after mixing was on the order of 1 to $5 \times 10^9\,cm^{-3}$, which is approximately 3 to 4 orders of magnitude above typical ambient OH concentrations.

Kovacs and Brune (2001) demonstrated that HO_2 radicals produced in the reactor via Reaction (R2) can regenerate OH at ambient NO mixing ratios above 1 ppbv. This secondary source of OH increases the OH concentration in the reactor, causing the OH decay to appear slower than it actually is, thus yielding a lower value of OH reactivity. These authors proposed a correction procedure for environments where NO is present at mixing ratios greater than 1 ppbv (Ren et al., 2003b), based on concomitant measurements of HO_2, OH and NO in the reactor. However, since the ambient daytime mixing ratios of NO during CABINEX were generally below

70 pptv with an average morning peak around 150 pptv, this correction was not necessary.

The OH detection system employs the FAGE technique for OH measurements, and is described in detail by Dusanter et al. (2009). Briefly, air from the reactor is sampled through a 1 mm pinhole and is expanded into a low-pressure cell held between 5 and 10 torr. This range of pressures is dependent on the orifice used with the FAGE inlet. With the orifice and pumping setup used during CABINEX, the pressure in the FAGE cell was 10.8 ± 0.5 torr. A tunable dye laser (Lambda Physik ScanMate 1) pumped by a Nd-YAG laser (Spectra Physics Navigator) operating at a pulse repetition rate of 5 kHz is used to produce coherent light at a wavelength of 616 nm. The frequency of this output is doubled with a BBO doubling crystal to produce radiation near 308 nm. A small fraction of the 308 nm light is sent to a reference cell, where a high concentration of OH is produced by thermal decomposition of water vapor. The resulting fluorescence signal is then detected by a photomultiplier tube and is used to determine when the wavelength of the laser is tuned in resonance with the $A^2\Sigma^+(v'=0) \leftarrow X^2\Pi(v''=0)$ electronic transition of OH. Approximately 38 % of the output from the laser is transmitted to the detection cell through a 2 m optical fiber (ThorLabs FG-200-UCR). The laser light then enters a multipass White cell and is reflected 20 times across the airstream. The resulting fluorescence is detected by a gated microchannel plate detector (Hamamatsu R5916U-52), and the signal is processed by a preamplifier (Advanced Instruments F100T) before being monitored by a photon counter (Stanford Research SRS 400).

A regenerative blower (Spencer VB001) connected to the adapter block pulls ambient air through the instrument at a flow rate of 175–$400\,L\,min^{-1}$ ($v \approx 150$–$350\,cm\,s^{-1}$), establishing turbulent flow conditions within the reactor with Reynolds numbers between 5000 and 11 000. Turbulent flow has several advantages over laminar flow conditions for measurements of reaction kinetics. In fully developed turbulent flows, exchange between the laminar sublayer at the walls of the reactor and the turbulent core is minimal (Seeley et al., 1993). This minimizes losses of VOCs and OH to the reactor

walls. Turbulent flow also promotes the mixing of VOCs and OH, which reduces the possibility of reactant segregation. To verify that the flow is turbulent within the reactor, flow velocity profiles were measured at the exit of the reactor with the Pitot tube. The flow velocity profile was measured approximately 2 cm upstream of the exit of the flow tube. Measurements of flow velocity were made at increments of 2 mm along the internal diameter of the flow tube. The flow velocity was uniform throughout the inner diameter of the flow tube for carrier gas flow rates above $100 \, \text{L} \, \text{min}^{-1}$, with a 10 % higher flow velocity at the center and sharp drop-offs near the wall of the flow tube. This profile matches the characteristics of turbulent flow as described by Seeley et al. (1993).

For ambient measurements, air is sampled through an 8.1 cm-i.d. hose constructed of perfluoroalkoxy (PFA) polymer film (thickness 0.13 mm) and attached to the ambient air intake. Different lengths of inlet tubing were used to sample at the various heights. A 14 m inlet was used for the 6 m measurements, while a 36 m inlet was used for the 21 and 31 m heights. The 14 and 36 m lengths of tubing resulted in residence times of air samples in the inlets of approximately 20 and 30 s, respectively, at the sampling flow rates used with each inlet during field measurements. To ensure that the inlet did not have an effect on the total OH reactivity measurements, various lengths of tubing (6–40 m) were attached to the flow tube reactor during laboratory experiments to change the residence time of air samples in the inlet (10–75 s) while measuring ambient OH reactivity at the same location. No statistically significant difference in OH reactivity was seen in these tests. A similar test was also performed in the field. For the CABINEX campaign, an additional inlet section (7 m long) was attached to a sampling inlet of 6.7 m, doubling the inlet length. The added section of inlet was alternately attached and removed every 30 min. The difference in reactivity between the 13.7 m inlet and the 6.7 m inlet was $0.32 \pm 0.5 \, \text{s}^{-1}$ ($n = 9$).

An automated linear motion system controls the movement of the OH injector. The injector is moved over a 37.5 cm path which starts 5 cm upstream of the FAGE detection inlet. The OH fluorescence signal is measured continuously (at a frequency of approximately 2 Hz) over the path of the injector in both the forward and reverse directions (Fig. 2). For the IU-TOHLM instrument, each OH decay measurement takes approximately 2.5 min to complete.

Under pseudo-first-order conditions (i.e., $[\text{OH}] \ll [\text{X}]$), the concentration of OH over time can be expressed as a first-order exponential decay:

$$[\text{OH}]_t = [\text{OH}]_0 \exp(-(k_{\text{OH}} + k_b) \, t). \qquad (3)$$

Solving Eq. (3) for the OH reactivity k_{OH} results in Eq. (4),

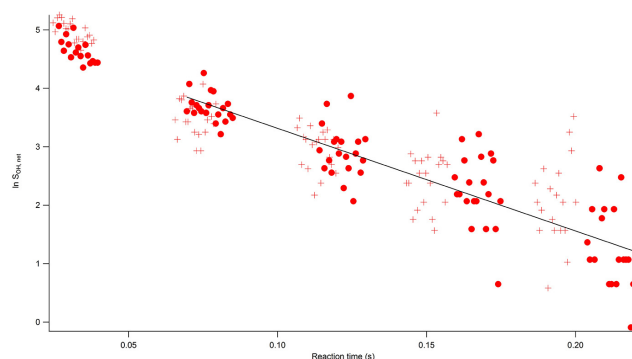$$k_{\text{OH}} = \frac{-\Delta(\ln[\text{OH}])}{\Delta t} - k_b, \qquad (4)$$

Fig. 2. Two subsequent OH decays from CABINEX, one measured with the injector traveling in the forward direction (crosses) and one measured with the injector traveling in the reverse direction (circles) on 10 July 2009. The solid line shows a linear fit yielding a value of OH reactivity of $16.4 \, \text{s}^{-1}$.

where k_b represents the OH loss rate due to wall reactions that is measured by flowing pure N_2 in the reactor. Note that dilution of OH in the core flow at the exit of the injector is also accounted for in k_b. Measurements of k_b were conducted both in the laboratory and in the field using nitrogen gas output from a liquid nitrogen dewar. Tests in the field were conducted on four separate days (see below). To test the effects of impurities from the carrier N_2 in the OH source on k_b, measurements of k_b were performed alternately with nitrogen from an industrial-grade N_2 dewar (Indiana Oxygen) and VOC-free nitrogen (purity of 99.9995 %, Matheson). The average difference between the k_b values from these two sources was $0.24 \, \text{s}^{-1}$, which corresponds to approximately 7 % of the k_b measured in these tests.

Measurements of k_b conducted in the laboratory exhibited similar relative variation to those conducted in the field. The day-to-day variability for the laboratory tests was approximately 10 % (from 1σ of $0.6 \, \text{s}^{-1}$), and the variation among the four field tests was approximately 8 % (from 1σ of $0.28 \, \text{s}^{-1}$). The average value of k_b for the field and laboratory tests was $3.6 \pm 0.2 \, \text{s}^{-1}$ ($n = 39$) for total flow rates between 130 and $200 \, \text{L} \, \text{min}^{-1}$, where the uncertainty represents one standard deviation of the average value. This value of k_b measured with the IU-TOHLM instrument is comparable to those reported previously for similar instruments (Kovacs and Brune, 2001; Mao et al., 2009; Ingham et al., 2009). The laboratory tests suggest that k_b may decrease with increasing flow rates in the reactor, and may be 1–$2 \, \text{s}^{-1}$ lower for flow rates higher than $200 \, \text{L} \, \text{min}^{-1}$. For the below-canopy measurements the average flow rate was approximately $220 \, \text{L} \, \text{min}^{-1}$, while for the above-canopy measurements, the average flow rate was approximately $350 \, \text{L} \, \text{min}^{-1}$. Unfortunately, measurements of k_b at flow rates greater than $200 \, \text{L} \, \text{min}^{-1}$ were not made in the field during CABINEX. As a result, the average value of k_b measured in these tests likely represents an upper limit to the background reactivity

for the above-canopy measurements, leading to a lower limit for the overall reactivity measured at 21 and 31 m.

Since the OH fluorescence signal is proportional to OH concentration, the net OH signal S_{OH} (the difference of the on-resonance and off-resonance OH fluorescence signals) can be substituted for [OH] in Eq. (4). Thus, the OH reactivity can be determined from the slope of a plot of the natural logarithm of S_{OH} as a function of reaction time (Fig. 2). Since the OH generated within the injector is still not completely mixed with the reactants in the reactor at short reaction times (< 50–60 ms), it is difficult to separate the OH loss due to dilution from the OH loss due to chemical reaction (Ingham et al., 2009). For this reason, analysis of the OH decays was started at a reaction time of 60 ms, when the injector was approximately 12 cm upstream of the FAGE inlet. However, this places an upper limit of 45 s^{-1} on the OH reactivity measurements with the IU-TOHLM instrument.

The accuracy and precision of the IU-TOHLM measurements were evaluated during laboratory experiments by measurements of the OH reactivity of four standard mixtures (propane, butane, tetramethylethylene (TME), and isoprene). These are representative of compounds that are present in ambient air and have well-established rate constant values spanning two orders of magnitude (10^{-12}–10^{-10} cm^3 molecule^{-1} s^{-1}) (Atkinson et al., 1995, 2006; Atkinson, 1997, 2003). A correlation plot of the measured and calculated OH reactivity (Fig. 3) shows that measurements are on average 38 % lower than calculated values when the measured velocity of the turbulent core is used to determine the reaction time. Similar discrepancies are observed for all the test compounds and suggest either an incomplete mixing between the reactants or a systematic underestimation of the reaction time. In addition, subsequent tests with trans-2-butene and propane showed similar behavior. Measured ambient OH reactivity values are scaled up by a factor determined from the fit shown in Fig. 3 to account for the average difference observed in these laboratory experiments. Given the similar behavior for all the test compounds, whose rate constants for reaction with OH span two orders of magnitude, and the linearity of the measured OH reactivity as a function of the calculated OH reactivity, it appears that this discrepancy does not vary with OH reactivity up to 35 s^{-1}. We therefore assume a linear scaling factor to account for the discrepancy.

The limit of detection (1σ), determined from measurements of k_b described above, is 0.7 s^{-1} under field conditions for a 10 min average. Measurements performed at multiple OH reactivity values indicate that the IU-TOHLM instrument can measure OH reactivity up to 45 s^{-1} with a 1σ precision of (1.2 s$^{-1} + 4$ % of the measured value) for a 10 min average.
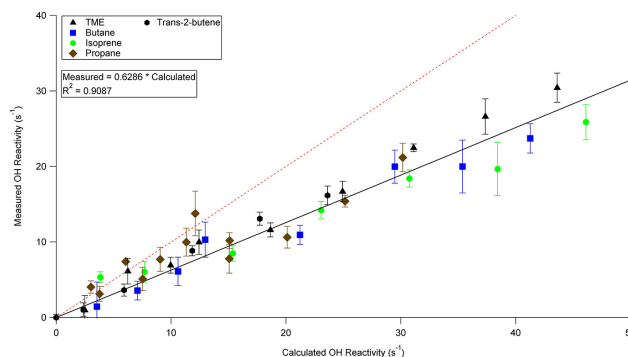

Fig. 3. Summary of laboratory characterizations of IU-TOHLM instrument. The dashed line represents the 1 : 1 line; the solid line is a linear fit of the data set represented by the solid markers. Error bars represent 1σ standard deviation of the average values.

2.2 Field measurements during CABINEX

The CABINEX field campaign was conducted from 1 July to 8 August 2009 at the PROPHET field site at the University of Michigan Biological Station in northern Michigan (Carroll et al., 2001). This site is located within a mixed deciduous forest with an average canopy height of 20 m. A previous study of the biomass within the area surrounding the site found an average of 156 ± 11 g m^{-2} of isoprene-emitting biomass, 90 % of which was attributed to aspen (Westberg, 2001).

The CABINEX campaign consisted of two phases; the first (1–20 July) focused on measurements below the forest canopy (6 m above ground level), and the second (21 July–8 August) focused on measurements above the forest canopy (21 and 31 m above ground level). Further details on the CABINEX campaign can be found in companion papers (Bryan et al., 2012; Griffith et al., 2013). Due to the limited instrumentation and variation in sampling schemes, the availability of collocated measurements varies among the different heights. Measurement techniques and their associated uncertainties are given in Table 2.

VOCs were measured with a proton transfer reaction mass spectrometer (PTR-MS) from Washington State University modified to incorporate dehumidified sampling for increased sensitivity toward formaldehyde (Jobson and McCoskey, 2010). The PTR-MS measurements include isoprene, the sum of methyl vinyl ketone and methacrolein (MVK + MACR), total monoterpenes, formaldehyde (HCHO), acetaldehyde, methanol, methyl hydroperoxide, acetone, methyl ethyl ketone, toluene, benzene, and the sum of C2-alkylbenzenes. The VOC measurements were alternated between the three heights (6, 21, and 31 m) at 10 min intervals.

Ambient temperature was measured with temperature probes (R. M. Young) placed at a height of 6 m on a trailer deployed by Washington State University and on the PROPHET tower at heights of 20.4 and 31.2 m. Ozone was

Table 2. Summary of supporting measurements from CABINEX used for OH reactivity calculations.

Measurement	Technique	Time resolution (min)/uncertainty (%, 1σ)/LOD (ppbv)	Institution
12 VOCs:	Proton transfer reaction mass spectrometry (PTR-MS)		Washington State University
Isoprene		1/5/0.05	
Methyl vinyl ketone + methacrolein		1/5/0.07	
Formaldehyde		1/10/0.14	
Acetaldehyde		1/5/0.09	
Acetone		1/5/0.12	
Methyl ethyl ketone		1/5/0.12	
Methanol		1/5/0.12	
Benzene		1/5/0.04	
Toluene		1/5/0.04	
Methyl peroxide		1/–*/0.05	
Total monoterpenes		1/5/0.07	
Ozone	UV absorption (Teledyne API 400E/Thermo Electron)	1/10/1	Indiana Univ./Univ. of Michigan
NO_2	Chemiluminescence (Air Quality Design)	1/12/0.002	Washington State University
CO	IR absorption (Thermo Electron 48C)	1/6/40	University of Michigan
Meteorological data: temperature, pressure		1/–/–	Washington State Univ. (6 m)
		1/–/–	University of Michigan (21 m, 31 m)
$J(NO_2)$	SAFS	1/30/–	University of Houston

* Uncertainty for methyl peroxide not yet quantified; refer to Jobson and McCoskey (2010) for further details.

measured by UV absorption using a Teledyne Model 400E. CO was measured by IR absorption using a Thermo Electron 48C by the University of Michigan in addition to ozone measurements using a Thermo Electron 49C instrument (Carroll et al., 2001). Nitrogen oxides ($NO_x = NO + NO_2$) were measured by Washington State University using an instrument based on chemiluminescence of NO and equipped with a blue light photolytic converter for NO_2 measurements (Air Quality Design). The NO_x measurements were alternated between the 6, 21, and 31 m heights in a similar manner to the VOC measurements. Photolysis frequencies for NO_2 were calculated from measurements made by the University of Houston with a scanning actinic flux spectroradiometer (SAFS) (Shetter et al., 2003) located at 32.6 m.

Measurements of total OH reactivity were made at three locations: below the forest canopy at a height of 6 m, approximately 1 m above the top of the canopy at a height of 21 m, and above the canopy at a height of 31 m. Approximately

17 days (5–21 July) were spent measuring total OH reactivity below the forest canopy, while measurements above the canopy were conducted on 18 days (22 July–8 August); this included four days of measurements at the 21 m level. Total OH reactivity was measured continuously with a time resolution of approximately 2.5 min, corresponding to the time required for measurement of a single OH decay. Measurements of the OH loss rate in N_2 (k_b in Eq. 4) were performed on 3 July, 10 July, 16 July, and 7 August.

3 Results

All relevant measurements, including total OH reactivity and ambient VOC mixing ratios, were averaged over a 10 min time step. Total OH reactivity was calculated from all measurements listed in Table 2. The temperature measured within the flow tube was used to calculate temperature-dependent rate constants. Furthermore, only
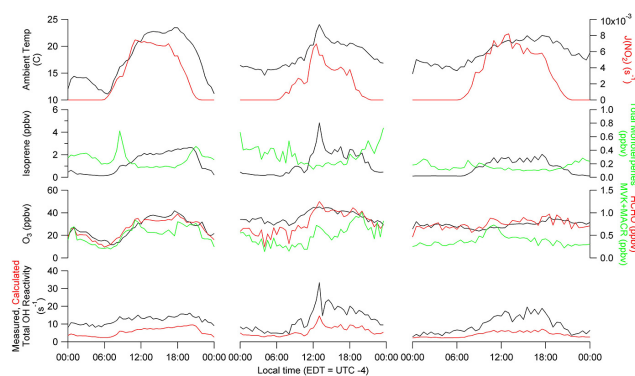
Fig. 4. Thirty min diurnal averages of measurements for the 6 m (left), 21 m (center), and 31 m (right) heights.
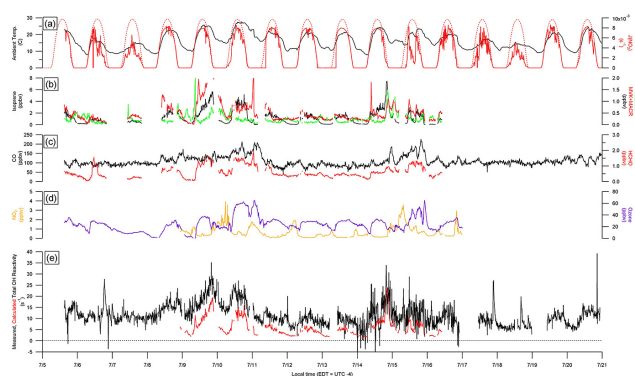

Fig. 5. Time series of 10 min averages for the 6 m height. The dashed line in panel a indicates values of $J(NO_2)$ calculated by the TUV 4.4 model for clear-sky conditions.

Fig. 6. Time series of 10 min averages for the 21 m height. The dashed line in panel a indicates values of $J(NO_2)$ calculated by the TUV 4.4 model for clear-sky conditions.

total OH reactivity measurements that were coincident with VOC and NO_x measurements are included in comparisons of measured and calculated OH reactivity. Measurements of ambient NO, SO_2, HONO, and glyoxal mixing ratios have not been used in the OH reactivity analysis, as their total contribution to the OH reactivity is less than $0.15 \, s^{-1}$.

Figure 4 shows the 30 min diurnal average values of ambient temperature, $J(NO_2)$ and OH reactivity, as well as ambient mixing ratios of ozone and some VOCs, at the 6, 21, and 31 m heights. Individual time series of the measurements are shown as Figs. 5–7. Figure 8 shows the 30 min diurnal average values of OH reactivity and the speciated contributions of trace gases for the 6, 21, and 31 m heights. Average ambient daytime temperatures from 12:00 to 18:00 span the same range of values among the three heights (20–26 °C, Fig. 4), although the average diurnal variation in temperature at 6 m (12.4 °C) is greater than that at 21 m (9.5 °C) or 31 m (7.2 °C) (Fig. 4, top panels). The magnitude of the measured OH reactivity was dependent on temperature, as the days with the highest ambient temperatures (20–25 °C) exhibited some of the highest measured OH reactivity (10, 24, 27 and 28 July) (Figs. 5–7, panel e).
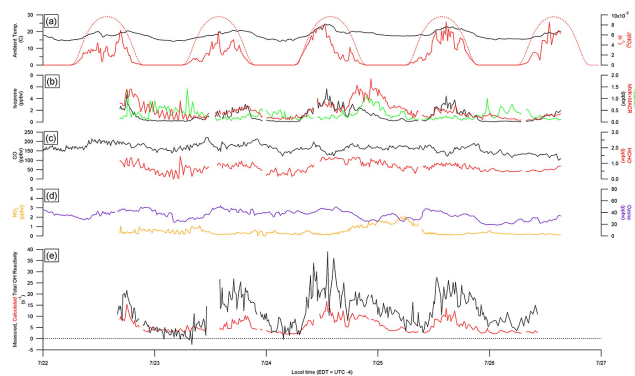
The measured OH reactivity at all heights shows a distinct diurnal trend, with diurnal averages ranging 8–16 s^{-1} at 6 m, 5–33 s^{-1} at 21 m, and 3–20 s^{-1} at 31 m (Fig. 4, bottom panels; Fig. 8). The diurnal trend in the measured OH reactivity is especially pronounced at the 21 m height. As expected in a site dominated by isoprene emissions (Westberg, 2001), isoprene was the dominant contributor to OH reactivity during the daytime hours, contributing 60–70 % of the calculated OH reactivity on average at all heights from 12:00 to 18:00 (Fig. 8). However, the contribution of isoprene decreased to 20–40 % when compared to the measured OH reactivity for the 21 and 31 m heights. Isoprene mixing ratios were similar at each height, with sustained daily maxima of around 2 ppbv, although there were several high-temperature events (7 July, 10 July, 24 July, 27 July) where the isoprene mixing ratios ranged from 4 to 6 ppbv (Figs. 5–7, panel b). Oxygenated VOCs (OVOCs, which include methyl vinyl ketone, methacrolein, methyl ethyl ketone, acetone, formaldehyde, acetaldehyde, methanol, and methyl peroxide) were the next largest contributor during the daytime, contributing 10–15 % to the calculated OH reactivity from 12:00 to 18:00. Among these, MVK + MACR was the largest contributor, accounting for 30 to 50 % of the OH reactivity from OVOCs during this time period. Mixing ratios of MVK + MACR were typically 0.25–1.0 ppbv on average at each height, with some diurnal variation, most evident at 6 m (Fig. 4). Typical HCHO mixing ratios were between 0.5 and 1.0 ppbv for all heights (Fig. 4), although the HCHO mixing ratio was close to 2.0 ppbv during the 27–28 July episode (Fig. 7, panel c).

Monoterpenes, oxygenated VOCs and CO were the dominant contributors to OH reactivity at night, each contributing roughly 20–30 % of the calculated OH reactivity on average from 00:00 to 06:00 and from 20:00 to 00:00 for all heights. Mixing ratios of monoterpenes were highest at night, approaching 1 ppbv at 6 m and 21 m, but less than 0.5 ppbv at 31 m (Figs. 5–7, panel b). Mixing ratios of CO showed very
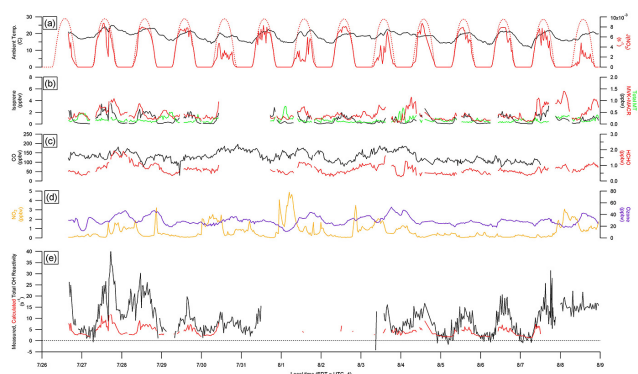
Fig. 7. Time series of 10 min averages for the 31 m height. The dashed line in panel a indicates values of $J(NO_2)$ calculated by the TUV 4.4 model for clear-sky conditions.
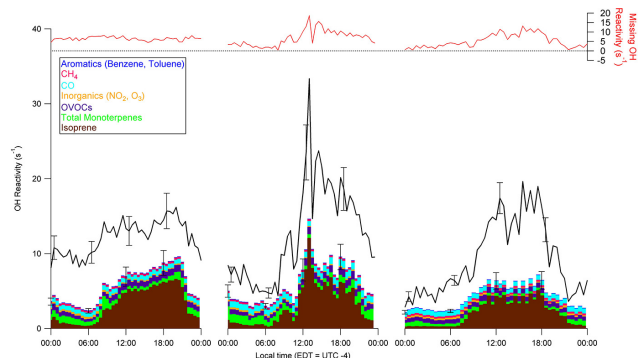

Fig. 8. Thirty min diurnal averages for OH reactivity at the 6 m (left), 21 m (center), and 31 m (right) heights. Measured OH reactivity is shown by the line; calculated OH reactivity is indicated by the colored bars. OVOCs include methyl vinyl ketone, methacrolein, MEK, acetone, formaldehyde, acetaldehyde, methanol, and methyl peroxide. Top plots show the missing reactivity at each height. Error bars on the calculated reactivity represent the uncertainty propagated from the 1σ uncertainties on the rate constants and concentrations of each species; error bars on the measured OH reactivity represent the 1σ uncertainty on a single OH reactivity measurement, propagated from uncertainties on measurements of flow velocity, injector distance, k_b, and the correction factor described in Sect. 2.1.

little diurnal variation, with an average mixing ratio on the order of 150 ppbv that approached 200 ppbv on some days.

The OH reactivity measured below the canopy at the 6 m height was generally lower than that measured above the canopy during the day (10:00–18:00), with an average missing OH reactivity of $6.2 \pm 0.2 \, s^{-1}$ (46 % of total; Figs. 4, 8). Missing reactivity was also observed at night (00:00–06:00, 22:00–00:00) at this height, with an average value of $6.5 \pm 0.2 \, s^{-1}$ (65 % of total). Above the canopy the average missing reactivity during the day (10:00–18:00) was on average $10.3 \pm 1 \, s^{-1}$ (48 % of total) for 21 m and $9.32 \pm 0.5 \, s^{-1}$ (61 % of total) for 31 m (Figs. 5–7, panel e). At night, the discrepancy between the measured and calculated reactivity

is smaller than during the day (Figs. 4, 8). These results suggest that there are additional sinks of OH that were not captured by the trace gas measurements.

The OH reactivity measurements and calculations were also binned by the ambient temperatures observed at each height (Fig. 9) to investigate the temperature dependence of OH reactivity contributions (Di Carlo et al., 2004; Mao et al., 2012). The width of each bin is 1 K, with the bin centered on the temperature of interest. At all heights, isoprene is the dominant contributor to the calculated OH reactivity at temperatures higher than 293 K, while monoterpenes and CO dominate the OH reactivity at temperatures lower than 291 K. The negative value at 284 K observed at 31 m likely reflects the overestimation of the background reactivity at this height as discussed above. The measurements at 31 m likely reflect a lower limit to the total OH reactivity (lower by $1–2 \, s^{-1}$). An inspection of Fig. 9 (top and center panels) indicates that the missing OH reactivity at 21 and 31 m exhibit a dependence on ambient temperature, with the missing reactivity increasing with increasing temperature. This trend is similar to that observed previously at this site during the PROPHET 2000 campaign (Di Carlo et al., 2004), although the magnitude of the missing OH reactivity is higher in this study. Di Carlo et al. (2004) observed $1–4 \, s^{-1}$ of missing reactivity over the temperature range of 286–298 K, whereas values up to 14 and $24 \, s^{-1}$ were observed for this study over the same temperature range for the 21 and 31 m heights, respectively. In contrast, the measurements below canopy at the 6 m height do not reveal a significant trend of missing reactivity with increasing temperature (Fig. 9, bottom panel).

4 Discussion

As mentioned above, Di Carlo et al. (2004) found that their measurements of total OH reactivity made during summer 2000 above the canopy at the PROPHET site were $1–4 \, s^{-1}$ greater than the OH reactivity calculated from measurements of the mixing ratios of OH sinks. From these observations, these authors suggested that emissions of an unmeasured highly reactive terpene could be responsible for the missing OH reactivity. However, subsequent measurements of total monoterpenes and sesquiterpenes at this site suggest that these compounds would only account for $0.7 \, s^{-1}$ of the reported missing OH reactivity, which corresponds to 30 % of the missing OH reactivity observed at 296 K during PROPHET 2000 (Kim et al., 2009).

Di Carlo et al. (2004) based their conclusions on the temperature dependence of the observed missing OH reactivity. The missing OH reactivity derived from these measurements was fitted with an equation often used to describe temperature-dependent emissions of monoterpenes (Guenther et al., 1993; Schade et al., 1999):
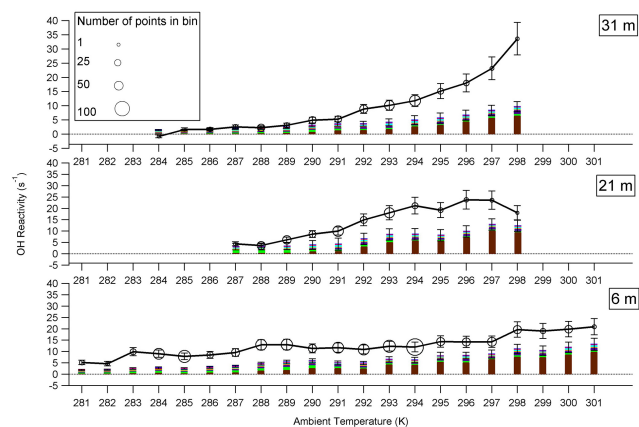
$$E(T) = E(293)\exp(\beta(T - 293)). \tag{5}$$

Fig. 9. Measured (lines, markers) and calculated (bars) total OH reactivity, binned by ambient temperature for the 6 m (bottom), 21 m (center), and 31 m (top) heights. The color scheme for the bars is the same as that for Fig. 8. Error bars on the calculated reactivity represent the uncertainty propagated from the 1σ uncertainties on the rate constants and concentrations of each species; error bars on the measured OH reactivity represent the 1σ uncertainty on a single OH reactivity measurement, propagated from uncertainties on measurements of flow velocity, injector distance, k_b, and the correction factor described in Sect. 2.1.

$E(T)$ represents the emission rate for a given temperature T. To compare the temperature dependence of the missing OH reactivity to the temperature dependence of monoterpene emissions described by Eq. (5), the temperature-dependent missing OH reactivity $MR(T)$ was substituted for $E(T)$ and $MR(293)$ for $E(293)$ in Eq. (5). Typical values for β, which is the factor representing the temperature dependence of the emission, range from 0.057 to 0.144 K^{-1} for a variety of monoterpenes, including α- and β-pinene, as well as limonene (Guenther et al., 1993). These values have been estimated from measurements of emission rates. The large variability in β is to be expected, as emission of monoterpenes can vary with plant species, location, and even among leaves on a specific plant. Experimental error can also factor into the variability in β (Guenther et al., 1993).

The missing OH reactivity measurements from the 2000 PROPHET campaign were fit to Eq. (5), resulting in a value for β of 0.11 (Di Carlo et al., 2004), a value similar to that previously observed for the temperature-dependent emission of Δ-3-carene (Schade et al., 1999). A similar treatment of the missing OH reactivity seen at the BEARPEX 2009 campaign, in which the missing OH reactivity is attributed to BVOC oxidation products, resulted in a β value of 0.17 (Mao et al., 2012), slightly higher than the upper limit of 0.144 K^{-1} observed for monoterpene emissions.

The missing OH reactivity data from CABINEX for the 21 and 31 m heights was also fit to Eq. (5). In contrast to the results described above, the values of β determined from the fits of the data for the 21 and 31 m heights (0.34 and 0.35, respectively) are not consistent with those observed
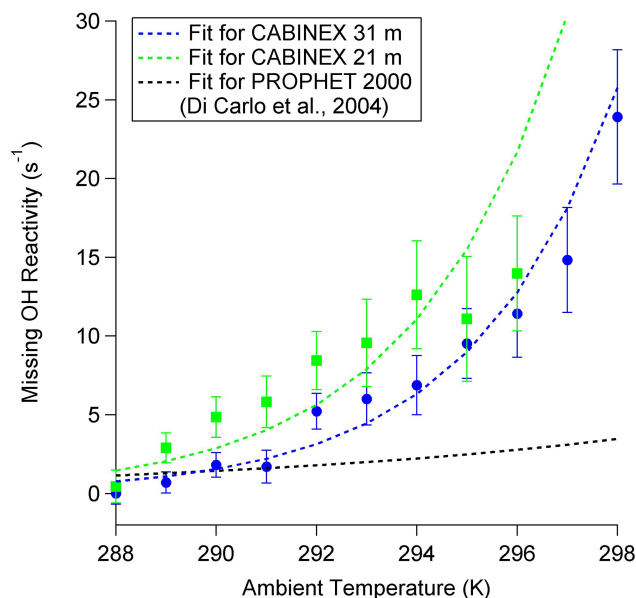

Fig. 10. Missing OH reactivity, binned by ambient temperature for the 21 m (squares) and 31 m (circles) heights for temperatures from 288 to 298 K. Dashed lines indicate fits to Eq. (5) for the 21 m height (green), 31 m height (blue), and the fit of the measurements from PROPHET 2000 reported by Di Carlo et al. (2004) (black). For the fits of the CABINEX data, MR(293) in Eq. (5) was determined from exponential fits of the measurements from 21 and 31 m. Due to the low number of points in the 297 and 298 K bins for the 21 m height, these points have not been included in the fit nor on this figure. Error bars represent the uncertainty (1σ) propagated from the uncertainties on individual measurements of OH reactivity (described in caption to Fig. 9) and the calculated OH reactivity.

during PROPHET 2000 and attributed to monoterpene emissions (Fig. 10). However, comparisons of β factors derived for monoterpene emissions must be made with caution, as β may not be the best metric for determination of the source of missing OH reactivity. Missing OH reactivity can be influenced by processes that do not affect BVOC emissions, such as boundary layer height and vertical mixing.

In addition, missing OH reactivity at the 31 m height does not appear to correlate with the measured mixing ratio of total monoterpenes (Fig. 11). These results are consistent with branch enclosure measurements of total OH reactivity during CABINEX that found that the measured OH reactivity was consistent with the calculated reactivity based on the measured VOC concentrations, including measurements of isoprene and monoterpene concentrations (Kim et al., 2011). These two findings indicate that directly emitted BVOCs are likely not the cause of the missing OH reactivity observed at this site.

The high missing OH reactivity measured during CABINEX at temperatures greater than 296 K is larger than the missing OH reactivity observed at these temperatures by Di Carlo et al. (2004) during the 2000 PROPHET campaign.
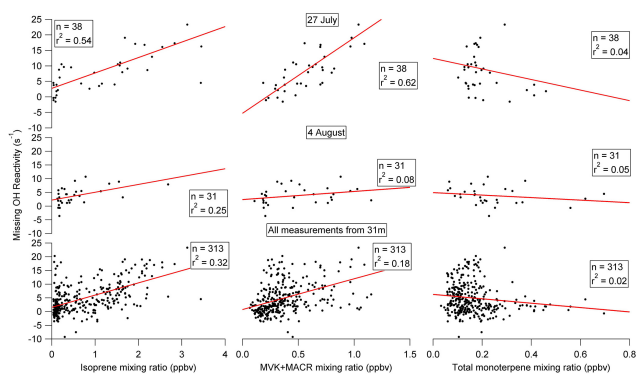
Fig. 11. Plots of missing OH reactivity from the 31 m height as a function of ambient isoprene, MVK + MACR, and total monoterpene mixing ratios for 27 July (top panels), 4 August (middle panels), and the entire 31 m data set (bottom panels).

However, the high missing OH reactivity observed during CABINEX at 31 m occurred during a two-day high temperature event (27–28 July, Fig. 7). The reason for the high measured missing OH reactivity during the 27–28 July episode is unclear, but may be related to either a transport event or a period of high photochemical activity, as the measured mixing ratio of HCHO was elevated during this event, with a peak mixing ratio of approximately 2 ppbv (Fig. 7, panel c, red trace) compared to an average value of 1 ppbv observed during the remaining 31 m measurement period (Fig. 4). Mixing ratios of isoprene during this episode were also 1–2 ppbv greater than the average values observed during the remaining measurement period at this height, as well as approximately 1 ppbv greater than the average daytime measurements during PROPHET 1998 (Apel et al., 2002), where conditions were similar to those during PROPHET 2000 (Di Carlo et al., 2004). The higher mixing ratios of isoprene could lead to higher concentrations of oxidation products, as the higher mixing ratios of MVK + MACR and formaldehyde suggest higher photochemical activity during this episode. Both of these possibilities will be explored further in a forthcoming paper (Hansen et al., 2014). It must be noted that many compounds are absent from the suite of measurements listed in Table 2, including C2-C4 alkenes and C2-C12 alkanes, some of which may be emitted by plants and soil (Kesselmeier and Staudt, 1999). These compounds were previously measured at this site during the PROPHET98 campaign with mixing ratios between 50 and 300 pptv. Depending on whether the median or maximum mixing ratios were used for the calculation, C2-C4 alkenes and C2-C12 alkanes could contribute 0.2 to 1.5 s^{-1} to the ambient OH reactivity. When other compounds from the 1998 data set (such as C5-C6 alkenes, substituted aromatics, and haloalkanes) were included, the range of OH reactivity contributed by these unmeasured compounds increases to 1.1 to 3.8 s^{-1}. This could account for 5 to 16 % of the missing OH reac-

tivity at 298 K and 31 m and 10 to 33 % of the missing OH reactivity at 296 K and 31 m.

Recent studies have suggested that unmeasured BVOC oxidation products from isoprene could explain some of the missing OH reactivity seen within isoprene-dominated environments (Karl et al., 2009; Kim et al., 2011). A time-dependent box model by Kim et al. (2011) for the PROPHET site found that first-generation unmeasured isoprene oxidation products could contribute approximately 7 % of the OH reactivity relative to the contribution of isoprene. These values correspond to approximately 8 % of the missing OH reactivity (at 298 K) observed by Di Carlo et al. (2004) and 2 % of the missing OH reactivity from the 31 m height (at 298 K) observed during CABINEX.

However, Karl et al. (2009) examined the chemistry of isoprene oxidation products in Amazonia using several models of isoprene chemistry. They found that isoprene oxidation products could account for a significant fraction of the total OH reactivity when the contribution of higher-generation oxidation products towards total OH reactivity was included. Depending on the exposure to OH, these models predicted that the overall OH reactivity from isoprene oxidation products could be as much as 150 % of the OH reactivity from isoprene. The results from this study suggest that unmeasured products from isoprene oxidation could explain a significant fraction of the missing OH reactivity seen above the canopy during CABINEX.

Figure 11 shows linear fits of the measured missing reactivity at the 31 m height as a function of the measured mixing ratios of isoprene, MVK + MACR, and total monoterpenes. Although the correlation coefficients are low, the results suggest that the missing reactivity is more likely related to isoprene and its oxidation products rather than monoterpene emissions. Although not shown, the linear regression of missing OH reactivity as a function of methyl peroxide mixing ratio is similar to that for the linear regression of missing OH reactivity as a function of MVK + MACR mixing ratio. The correlation coefficient for the fit of the observed missing OH reactivity as a function of MVK + MACR mixing ratio is higher on 27 July ($R^2 = 0.62$), when the missing OH reactivity is high (Fig. 11, top), than on a day when the missing OH reactivity is low such as on 4 August (Fig. 11, center) ($R^2 = 0.08$). These results suggest that the missing OH reactivity observed on 27–28 July may have been enhanced by unmeasured BVOC oxidation products due to more efficient photochemistry during this period. Future work will involve estimating the contribution of unmeasured oxidation products from isoprene, monoterpenes, and sesquiterpenes to the total OH reactivity through model simulations incorporating the explicit chemistry included in the Master Chemical Mechanism, version 3.2 (Hansen et al., 2014).

Although missing OH reactivity was observed above the forest canopy during CABINEX for temperatures greater than 293 K, the OH reactivity observed below the canopy over the same temperature range is in better agreement with

the calculated reactivity (Fig. 9). However, the mixing ratios of measured VOCs and inorganic trace species were found to be similar among the three heights, including the mixing ratios of isoprene oxidation products such as MVK + MACR (Figs. 5–7). Thus, given the similar composition above and below the canopy, one would expect to observe missing OH reactivity at 6 m that was comparable in magnitude to that observed at 21 and 31 m. It should be noted that there was one episode of significant high missing OH reactivity at the 6 m height that occurred on 10 July (Fig. 5, panel e). As in the episode on 27–28 July at 31 m, the mixing ratios of isoprene and MVK+MACR were elevated on this day, with daytime mixing ratios of isoprene approximately 4 ppbv (Fig. 5, panel b), and daytime MVK + MACR mixing ratios approximately 0.75 ppbv (Fig. 5, panel b). In addition, NO_2 mixing ratios were elevated (1–2 ppbv, Fig. 5, panel d) in the early morning. This again suggests that the elevated OH reactivity was the result of either a transport event or a period of elevated photochemical activity.

It is possible that some of the BVOC oxidation products suspected of being the source of the missing OH reactivity above the canopy were lost to deposition within the forest canopy during turbulent mixing. A study incorporating ecosystem-scale flux measurements from six field campaigns has shown that dry deposition onto vegetation represents a significant loss of oxygenated VOCs in forested environments (Karl et al., 2010). Furthermore, an examination of vertical deposition profiles indicates that almost all (> 97 %) of the deposition of oxygenated VOCs occurs in the upper 70 % of the forest canopy. For most of the species investigated (hydroxyacetone, C4-carbonyls, glycolaldehyde, nopinone, MVK+MACR), the dry deposition velocities were greater than $1 \, cm \, s^{-1}$ within this regime. Modeling studies incorporating 1-D models such as the one used in Bryan et al. (2012) and Mogensen et al. (2011) would also be useful to test whether deposition processes are efficient enough to remove oxygenated species from air masses injected within and below the canopy.

In contrast to the measurements made above the canopy, significant missing reactivity was observed below canopy at night when temperatures were below approximately 293 K (Figs. 4, 5, 8, 9). Missing OH reactivity was also observed at low temperatures at the top of the forest canopy during the BEARPEX 2007 field campaign (Wolfe et al., 2011); this was attributed to a missing source of formaldehyde. A modeling study of a boreal forest performed by Mogensen et al. (2011) suggests that summertime OH reactivity is higher below the canopy during the night but decreases during the day due to efficient mixing, in contrast to measurements at this site (Sinha et al., 2010). The missing OH reactivity seen below the canopy during CABINEX may be due to enhanced oxidation of mono- and sesquiterpene emissions in the stable nighttime boundary layer producing unmeasured oxidation products that accumulate below the forest canopy due to suppressed turbulent mixing, or oxidation products produced during the day that are trapped below the canopy at night. However, in contrast to the above-canopy observations, the missing reactivity observed below the canopy does not exhibit any consistent trend with the mixing ratios of isoprene, MVK + MACR, or monoterpenes (Fig. S3), even though some of the periods of greatest missing reactivity occurred during periods when the mixing ratio of ozone below the canopy was high (9 and 10 July, Fig. 5). Additional measurements of OH reactivity and biogenic VOCs below the forest canopy are needed to determine the source of this missing reactivity. Because these measurements of OH reactivity were performed during three different time periods of varying duration, measurements of OH reactivity with rapid switching between heights will be necessary to confirm these results.

5 Conclusions

Measured total OH reactivity above the forest canopy during the CABINEX campaign was significantly greater than that calculated based on measurements of the concentration of OH sinks, similar to that observed previously at this site. However, in contrast to these previous results, the measured missing OH reactivity in this study is not consistent with the emission of unmeasured BVOCs. Instead, the missing OH reactivity observed above the canopy may be due to unmeasured oxidation products, consistent with other studies (Karl et al., 2009; Kim et al., 2011; Edwards et al., 2013). A comprehensive modeling study focusing on VOC oxidation above the forest canopy is necessary to determine whether secondary species formed during the oxidation of isoprene are present at concentrations that are high enough to explain the missing OH reactivity observed in this study, or whether additional reactive gases are necessary to explain these observations. This work will be the focus of an upcoming publication (Hansen et al., 2014).

In contrast, the missing OH reactivity observed below the forest canopy for temperatures greater than approximately 293 K was in better agreement with the calculated reactivity based on measurements of isoprene, monoterpenes, and a few BVOC oxidation products such as methacrolein, methyl vinyl ketone, and formaldehyde. Although the concentrations of some oxidation products below canopy such as MVK + MACR are similar to those observed above canopy due to efficient in-canopy mixing (Bryan et al., 2012), species responsible for the missing OH reactivity above the canopy may be lost to deposition within the forest canopy and may not contribute to the OH reactivity at the 6 m height. Less efficient mixing below the canopy may also trap oxidation products produced at the 6 m height. However, as the measurements at the three heights were performed at different time periods, the influence of other factors between these heights cannot be ruled out. Additional 1-D modeling of deposition processes within and below the canopy as

well as additional sequential measurements of OH reactivity and associated OVOCs both above and below forest canopies would be useful to confirm the results presented in this study.

Supplementary material related to this article is available online at http://www.atmos-chem-phys.net/14/2923/2014/acp-14-2923-2014-supplement.pdf.

References

Apel, E. C., Riemer, D. D., Hills, A., Baugh, W., Orlando, J., Faloona, I., Tan, D., Brune, W., Lamb, B., Westberg, H., Carroll, M. A., Thornberry, T., and Geron, C. D.: Measurement and interpretation of isoprene fluxes and isoprene, methacrolein, and methyl vinyl ketone mixing ratios at the PROPHET site during the 1998 intensive, J. Geophys. Res., 107, 4034, doi:10.1029/2000JD000225, 2002.

Atkinson, R.: Gas-Phase Tropospheric Chemistry of Volatile Organic Compounds: 1. Alkanes and Alkenes, J. Phys. Chem. Ref. Data, 26, 215–290, 1997.

Atkinson, R.: Kinetics of the gas-phase reactions of OH radicals with alkanes and cycloalkanes, Atmos. Chem. Phys., 3, 2233–2307, doi:10.5194/acp-3-2233-2003, 2003.

Atkinson, R., Arey, J., Aschmann, S. M., Corchnoy, S. B., and Shu, Y.: Rate Constants for the Gas-Phase Reactions of *cis*-3-Hexen-1-ol, *cis*-3-Hexenylacetate, *trans*-2-Hexenal, and Linalool with OH and NO_3 Radicals and O_3 at $296 \pm 2K$, and OH Radical Formation Yields from the O_3 Reactions, Int. J. Chem. Kinet., 27, 941–955, 1995.

Atkinson, R., Baulch, D. L., Cox, R. A., Crowley, J. N., Hampson, R. F., Hynes, R. G., Jenkin, M. E., Rossi, M. J., Troe, J., and IUPAC Subcommittee: Evaluated kinetic and photochemical data for atmospheric chemistry: Volume II – gas phase reactions of organic species, Atmos. Chem. Phys., 6, 3625–4055, doi:10.5194/acp-6-3625-2006, 2006.

Bryan, A. M., Bertman, S. B., Carroll, M. A., Dusanter, S., Edwards, G. D., Forkel, R., Griffith, S., Guenther, A. B., Hansen, R. F., Helmig, D., Jobson, B. T., Keutsch, F. N., Lefer, B. L., Pressley, S. N., Shepson, P. B., Stevens, P. S., and Steiner, A. L.: In-canopy gas-phase chemistry during CABINEX 2009: sensitivity of a 1-D canopy model to vertical mixing and isoprene chemistry, Atmos. Chem. Phys., 12, 8829–8849, doi:10.5194/acp-12-8829-2012, 2012.

Carroll, M. A., Bertman, S. B., and Shepson, P. B.: Overview of the Program on Research for Oxidants: PHotochemistry, Emissions,

and Transport (PROPHET) 1998 summer intensive, J. Geophys. Res., 106, 24275–24288, 2001.

Chatani, S., Shimo, N., Matsunaga, S., Kajii, Y., Kato, S., Nakashima, Y., Miyazaki, K., Ishii, K., and Ueno, H.: Sensitivity analyses of OH missing sinks over Tokyo metropolitan area in the summer of 2007, Atmos. Chem. Phys., 9, 8975–8986, doi:10.5194/acp-9-8975-2009, 2009.

Di Carlo, P., Brune, W. H., Martinez, M., Harder, H., Lesher, R., Ren, X., Thornberry, T., Carroll, M. A., Young, V., Shepson, P. B., Reimer, D., Apel, E., and Campbell, C.: Missing OH Reactivity in a Forest: Evidence for Unknown Reactive Biogenic VOCs, Science, 304, 722–725, 2004.

Dolgorouky, C., Gros, V., Sarda-Esteve, R., Sinha, V., Williams, J., Marchand, N., Sauvage, S., Poulain, L., Sciare, J., and Bonsang, B.: Total OH reactivity measurements in Paris during the 2010 MEGAPOLI winter campaign, Atmos. Chem. Phys., 12, 9593–9612, doi:10.5194/acp-12-9593-2012, 2012.

Dusanter, S., Vimal, D., and Stevens, P. S.: Technical note: Measuring tropospheric OH and HO_2 by laser-induced fluorescence at low pressure. A comparison of calibration techniques, Atmos. Chem. Phys., 8, 321–340, doi:10.5194/acp-8-321-2008, 2008.

Dusanter, S., Vimal, D., Stevens, P. S., Volkamer, R., and Molina, L. T.: Measurements of OH and HO_2 concentrations during the MCMA-2006 field campaign – Part 1: Deployment of the Indiana University laser-induced fluorescence instrument, Atmos. Chem. Phys., 9, 1665–1685, doi:10.5194/acp-9-1665-2009, 2009.

Edwards, P. M., Evans, M. J., Furneaux, K. L., Hopkins, J., Ingham, T., Jones, C., Lee, J. D., Lewis, A. C., Moller, S. J., Stone, D., Whalley, L. K., and Heard, D. E.: OH reactivity in a South East Asian tropical rainforest during the Oxidant and Particle Photochemical Processes (OP3) project, Atmos. Chem. Phys., 13, 9497–9514, doi:10.5194/acp-13-9497-2013, 2013.

Ehhalt, D. H.: Atmospheric chemistry – Radical ideas, Science, 279, 1002–1003, 1998.

Goldstein, A. H. and Galbally, I. E.: Known and unexplored organic constituents in the earth's atmosphere, Environ. Sci. Technol., 41, 1514–1521, 2007.

Griffith, S. M., Hansen, R. F., Dusanter, S., Stevens, P. S., Alaghmand, M., Bertman, S. B., Carroll, M. A., Erickson, M., Galloway, M., Grossberg, N., Hottle, J., Hou, J., Jobson, B. T., Kammrath, A., Keutsch, F. N., Lefer, B. L., Mielke, L. H., O'Brien, A., Shepson, P. B., Thurlow, M., Wallace, W., Zhang, N., and Zhou, X. L.: OH and HO_2 radical chemistry during PROPHET 2008 and CABINEX 2009 –Part 1: Measurements and model comparison, Atmos. Chem. Phys., 13, 5403–5423, doi:10.5194/acp-13-5403-2013, 2013.

Guenther, A. B., Zimmerman, P. R., Harley, P. C., Monson, R. K., and Fall, R.: Isoprene and Monoterpene Emission Rate Variability – Model Evaluations and Sensitivity Analyses, J. Geophys. Res.-Atmos., 98, 12609–12617, 1993.

Hansen, R. F., Griffith, S. M., Dusanter, S., Stevens, P. S., Bertman, S. B., Bryan, A. M., Carroll, M. A., Erickson, M. H., Flynn, J. H., Galloway, M. M., Grossberg, N., Hou, J., Jobson, B. T., Keutsch, F. N., Lefer, B. L., O'Brien, A., Shepson, P. B., Steiner, A. L., Thurlow, M., Wallace, H. W., Zhang, N., and Zhou, X. L.: Measurements of Total Hydroxyl Radical Reactivity during the CABINEX 2009 Field Campaign: Part 2 – Modeling of Hydroxyl Radical Reactivity, Atmos. Chem. Phys., in preparation, 2014.

Holzinger, R., Lee, A., Paw, K. T., and Goldstein, U. A. H.: Observations of oxidation products above a forest imply biogenic emissions of very reactive compounds, Atmos. Chem. Phys., 5, 67–75, doi:10.5194/acp-5-67-2005, 2005.

Ingham, T., Goddard, A., Whalley, L. K., Furneaux, K. L., Edwards, P. M., Seal, C. P., Self, D. E., Johnson, G. P., Read, K. A., Lee, J. D., and Heard, D. E.: A flow-tube based laser-induced fluorescence instrument to measure OH reactivity in the troposphere, Atmos. Meas. Tech., 2, 465–477, doi:10.5194/amt-2-465-2009, 2009.

Jobson, B. T. and McCoskey, J. K.: Sample drying to improve HCHO measurements by PTR-MS instruments: laboratory and field measurements, Atmos. Chem. Phys., 10, 1821–1835, doi:10.5194/acp-10-1821-2010, 2010.

Karl, T., Guenther, A., Turnipseed, A., Tyndall, G., Artaxo, P., and Martin, S.: Rapid formation of isoprene photo-oxidation products observed in Amazonia, Atmos. Chem. Phys., 9, 7753–7767, doi:10.5194/acp-9-7753-2009, 2009.

Karl, T., Harley, P., Emmons, L., Thornton, B., Guenther, A., Basu, C., Turnipseed, A., and Jardine, K.: Efficient Atmospheric Cleansing of Oxidized Organic Trace Gases by Vegetation, Science, 330, 816–819, 2010.

Kesselmeier, J. and Staudt, M.: Biogenic Volatile Organic Compounds (VOC): An Overview on Emission, Physiology, and Ecology, J. Atmos. Chem., 33, 23–88, 1999.

Kim, S., Karl, T., Helmig, D., Daly, R., Rasmussen, R., and Guenther, A.: Measurement of atmospheric sesquiterpenes by proton transfer reaction-mass spectrometry (PTR-MS), Atmos. Meas. Tech., 2, 99–112, doi:10.5194/amt-2-99-2009, 2009.

Kim, S., Guenther, A., Karl, T., and Greenberg, J.: Contributions of primary and secondary biogenic VOC tototal OH reactivity during the CABINEX (Community Atmosphere-Biosphere INteractions Experiments)-09 field campaign, Atmos. Chem. Phys., 11, 8613–8623, doi:10.5194/acp-11-8613-2011, 2011.

Kovacs, T. A. and Brune, W. H.: Total OH Loss Rate Measurement, J. Atmos. Chem., 39, 105–122, 2001.

Kovacs, T. A., Brune, W. H., Harder, H., Martinez, M., Simpas, J. B., Frost, G. J., Williams, E., Jobson, T., Stroud, C., Young, V., Fried, A., and Wert, B.: Direct measurements of urban OH reactivity during Nashville SOS in summer 1999, J. Environ. Monitor., 5, 68–74, 2003.

Lou, S., Holland, F., Rohrer, F., Lu, K., Bohn, B., Brauers, T., Chang, C. C., Fuchs, H., Häseler, R., Kita, K., Kondo, Y., Li, X., Shao, M., Zeng, L., Wahner, A., Zhang, Y., Wang, W., and Hofzumahaus, A.: Atmospheric OH reactivities in the Pearl River Delta – China in summer 2006: measurement and model results, Atmos. Chem. Phys., 10, 11243–11260, doi:10.5194/acp-10-11243-2010, 2010.

Mao, J., Ren, X., Brune, W. H., Olson, J. R., Crawford, J. H., Fried, A., Huey, L. G., Cohen, R. C., Heikes, B., Singh, H. B., Blake, D. R., Sachse, G. W., Diskin, G. S., Hall, S. R., and Shetter, R. E.: Airborne measurement of OH reactivity during INTEX-B, Atmos. Chem. Phys., 9, 163–173, doi:10.5194/acp-9-163-2009, 2009.

Mao, J., Ren, X., Chen, S., Brune, W. H., Chen, Z., Martinez, M., Harder, H., Lefer, B., Rappenglück, B., Flynn, J., and Leuchner, M.: Atmospheric oxidation capacity in the summer of Houston 2006: Comparison with summer measurements in other metropolitan studies, Atmos. Environ., 44, 4107–4115, 2010.

Mao, J., Ren, X., Zhang, L., Van Duin, D. M., Cohen, R. C., Park, J.-H., Goldstein, A. H., Paulot, F., Beaver, M. R., Crounse, J. D., Wennberg, P. O., DiGangi, J. P., Henry, S. B., Keutsch, F. N., Park, C., Schade, G. W., Wolfe, G. M., Thornton, J. A., and Brune, W. H.: Insights into hydroxyl measurements and atmospheric oxidation in a California forest, Atmos. Chem. Phys., 12, 8009–8020, doi:10.5194/acp-12-8009-2012, 2012.

Mogensen, D., Smolander, S., Sogachev, A., Zhou, L., Sinha, V., Guenther, A., Williams, J., Nieminen, T., Kajos, M. K., Rinne, J., Kulmala, M., and Boy, M.: Modelling atmospheric OH-reactivity in a boreal forest ecosystem, Atmos. Chem. Phys., 11, 9709–9719, doi:10.5194/acp-11-9709-2011, 2011.

Nölscher, A. C., Williams, J., Sinha, V., Custer, T., Song, W., Johnson, A. M., Axinte, R., Bozem, H., Fischer, H., Pouvesle, N., Phillips, G., Crowley, J. N., Rantala, P., Rinne, J., Kulmala, M., Gonzales, D., Valverde-Canossa, J., Vogel, A., Hoffmann, T., Ouwersloot, H. G., Vilà-Guerau de Arellano, J., and Lelieveld, J.: Summertime total OH reactivity measurements from boreal forest during HUMPPA-COPEC 2010, Atmos. Chem. Phys., 12, 8257–8270, doi:10.5194/acp-12-8257-2012, 2012.

Ren, X., Harder, H., Martinez, M., Lesher, R. L., Oliger, A., Shirley, T., Adams, J., Simpas, J. B., and Brune, W. H.: HO$_X$ concentrations and OH reactivity observations in New York City during PMTACS-NY2001, Atmos. Environ., 37, 3627–3637, 2003a.

Ren, X., Harder, H., Martinez, M., Lesher, R. L., Oliger, A., Simpas, J. B., Brune, W. H., Schwab, J. J., Demerjian, K. L., He, Y., Zhou, X. L., and Gao, H. G.: OH and HO$_2$ chemistry in the urban atmosphere of New York City, Atmos. Environ., 37, 3639–3651, 2003b.

Ren, X., Brune, W. H., Mao, J. Q., Mitchell, M. J., Lesher, R. L., Simpas, J. B., Metcalf, A. R., Schwab, J. J., Cai, C. X., Li, Y. Q., Demerjian, K. L., Felton, H. D., Boynton, G., Adams, A., Perry, J., He, Y., Zhou, X. L., and Hou, J.: Behavior of OH and HO$_2$ in the winter atmosphere in New York city, Atmos. Environ., 40, 252–263, 2006a.

Ren, X., Brune, W. H., Oliger, A., Metcalf, A. R., Simpas, J. B., Shirley, T., Schwab, J. J., Bai, C., Roychowdhury, U., Li, Y., Cai, C., Demerjian, K. L., He, Y., Zhou, X., Gao, H., and Hou, J.: OH, HO$_2$, and OH reactivity during the PMTACS-NY Whiteface Mountain 2002 campaign: Observations and model comparison, J. Geophys. Res., 111, D10S03, doi:10.1029/2005JD006126, 2006b.

Sadanaga, Y., Yoshino, A., Kato, S., Yoshioka, A., Watanabe, K., Miyakawa, Y., Hayashi, I., Ichikawa, M., Matsumoto, J., Nishiyama, A., Akiyama, N., Kanaya, Y., and Kajii, Y.: The importance of NO$_2$ and volatile organic compounds in the urban air from the viewpoint of the OH reactivity, Geophys. Res. Lett., 31, L08102, doi:10.1029/2004gl019661, 2004a.

Sadanaga, Y., Yoshino, A., Watanabe, K., Yoshioka, A., Wakazono, Y., Kanaya, Y., and Kajii, Y.: Development of a Measurement System of OH reactivity in the atmosphere by using a laser-induced pump and probe technique, Rev. Sci. Instrum., 75, 2648–2655, 2004b.

Schade, G. W., Goldstein, A. H., and Lamanna, M. S.: Are monoterpene emissions influenced by humidity?, Geophys. Res. Lett., 26, 2187–2190, 1999.

Seeley, J. V., Jayne, J. T., and Molina, M. J.: High-Pressure Fast-Flow Technique for Gas Kinetics Studies, Int. J. Chem. Kinet., 25, 571–594, 1993.

Shetter, R. E., Junkermann, W., Swartz, W. H., Frost, G. J., Craw-ford, J. H., Lefer, B. L., Barrick, J. D., Hall, S. R., Hofzuma-haus, A., Bais, A., Calvert, J. G., Cantrell, C. A., Madronich, S., Muller, M., Kraus, A., Monks, P. S., Edwards, G. D., McKenzie, R., Johnston, P., Schmitt, R., Griffioen, E., Krol, M., Kylling, A., Dickerson, R. R., Lloyd, S. A., Martin, T., Gar-diner, B., Mayer, B., Pfister, G., Roth, E. P., Koepke, P., Rug-gaber, A., Schwander, H., and van Weele, M.: Photolysis fre-quency of NO_2: Measurement and modeling during the Inter-national Photolysis Frequency Measurement and Modeling In-tercomparison (IPMMI), J. Geophys. Res.-Atmos., 108, 8544, doi:10.1029/2002JD002932, 2003.

Sinha, V., Williams, J., Crowley, J. N., and Lelieveld, J.: The Com-parative Reactivity Method – a new tool to measure total OH Reactivity in ambient air, Atmos. Chem. Phys., 8, 2213–2227, doi:10.5194/acp-8-2213-2008, 2008.

Sinha, V., J., W., Lelieveld, J., Ruuskanen, T. M., Kajos, M. K., Patokoski, J., Hellen, H., Hakola, H., Mogensen, D., Boy, M., Rinne, J., and Kumala, M.: OH Reactivity Measurements within a Boreal Forest: Evidence for Unknown Reactive Emissions, En-viron. Sci. Technol., 44, 6614–6620, 2010.

Sinha, V., Williams, J., Diesch, J. M., Drewnick, F., Martinez, M., Harder, H., Regelin, E., Kubistin, D., Bozem, H., Hosaynali-Beygi, Z., Fischer, H., Andrés-Hernández, M. D., Kartal, D., Adame, J. A., and Lelieveld, J.: Constraints on instantaneous ozone production rates and regimes during DOMINO derived using in-situ OH reactivity measurements, Atmos. Chem. Phys., 12, 7269–7283, doi:10.5194/acp-12-7269-2012, 2012.

Westberg, H., Lamb, B., Hafer, R., Hills, A., Shepson, P., and Vo-gel, C.: Measurement of isoprene fluxes at the PROPHET site, J. Geophys. Res., 106, 24347–24358, 2001.

Wolfe, G. M., Thornton, J. A., Bouvier-Brown, N. C., Goldstein, A. H., Park, J.-H., McKay, M., Matross, D. M., Mao, J., Brune, W. H., LaFranchi, B. W., Browne, E. C., Min, K.-E., Wooldridge, P. J., Cohen, R. C., Crounse, J. D., Faloona, I. C., Gilman, J. B., Kuster, W. C., de Gouw, J. A., Huisman, A., and Keutsch, F. N.: The Chemistry of Atmosphere-Forest Exchange (CAFE) Model – Part 2: Application to BEARPEX-2007 observations, Atmos. Chem. Phys., 11, 1269–1294, doi:10.5194/acp-11-1269-2011, 2011.

Yoshino, A., Sadanaga, Y., Watanabe, K., Kato, S., Miyakawa, Y., Matsumoto, J., and Kajii, Y.: Measurement of total OH reactiv-ity by laser-induced pump and probe technique – comprehensive observations in the urban atmosphere of Tokyo, Atmos. Environ., 40, 7869–7881, 2006.